THE JOURNAL OF PHYSICAL CHEMISTRY B

Subscriber access provided by OAK RIDGE NATIONAL LAB

Article

Structural Investigation of PAMAM Dendrimers in Aqueous Solutions Using Small-Angle Neutron Scattering: Effect of Generation

Lionel Porcar, Yun Liu, Rafael Verduzco, Kunlun Hong, Paul D. Butler, Linda J. Magid, Gregory S. Smith, and Wei-Ren Chen

J. Phys. Chem. B, **2008**, 112 (47), 14772-14778 • Publication Date (Web): 25 October 2008

Downloaded from http://pubs.acs.org on November 24, 2008

More About This Article

Additional resources and features associated with this article are available within the HTML version:

- Supporting Information
- Access to high resolution figures
- Links to articles and content related to this article
- Copyright permission to reproduce figures and/or text from this article

View the Full Text HTML

ACS Publications
High quality. High impact.

The Journal of Physical Chemistry B is published by the American Chemical Society. 1155 Sixteenth Street N.W., Washington, DC 20036

Structural Investigation of PAMAM Dendrimers in Aqueous Solutions Using Small-Angle Neutron Scattering: Effect of Generation

Lionel Porcar,[†,‡,§] Yun Liu,[‡,§] Rafael Verduzco,[||] Kunlun Hong,[||] Paul D. Butler,[§,⊥] Linda J. Magid,[⊥] Gregory S. Smith,[#] and Wei-Ren Chen*[,#]

Institut Laue-Langevin, B.P. 156, F-38042 Grenoble Cedex 9, France; The NIST Center for Neutron Research, National Institute of Standards and Technology, Gaithersburg, Maryland 20899-6100; Department of Materials Science and Engineering, University of Maryland, College Park, Maryland 20742; The Center for Nanophase Materials Sciences, Oak Ridge National Laboratory, Oak Ridge, Tennessee 37831; Department of Chemistry, the University of Tennessee, Knoxville, Tennessee 37996-1600; and Neutron Scattering Science Division, Spallation Neutron Source, Oak Ridge National Laboratory, Oak Ridge, Tennessee 37831

Received: June 16, 2008; Revised Manuscript Received: August 20, 2008

We investigate a series of poly(amidoamine) starburst dendrimers (PAMAM) of different generations in acidic, aqueous solutions using small-angle neutron scattering (SANS). While the overall molecular size is found to be practically unaffected by a pD change, a strong generational dependence of counterion association is revealed. Upon increasing the dendrimer generation, the effective charge obtained from our SANS experiments only shows a small increase in contrast to the nearly exponential increase predicted by a recent atomic simulation. We also find that with the same degree of molecular protonation *the specific counterion association*, which is defined as the ratio of bound chloride anions to positively charged amines in solutions, is larger for higher-generation PAMAM dendrimer. The associated counterion density also increases upon increasing generation number.

I. Introduction

Dendrimers are polymers with a tree-like structure that combine properties of both polymers and hard-sphere colloids. They are spherical in shape like most colloids, but they also possess some internal degrees of freedom due to their polymer-like nature, which results in a rich and complex structures and dynamic behaviors.[1] In addition to the fundamental scientific interest in understanding the consequences of this polymer–colloid duality, dendrimer science is driven by the potential use of dendrimers as novel biomedical agents.[2] It became obvious that the key parameter for optimizing dendrimers for biomedical applications is understanding, controlling, and optimizing their intra- and intermolecular structure in aqueous environments with various acidity and ionic strength. However, a quantitative and pertinent physical description of the dendrimer behavior in solution is still lacking not only experimentally but also theoretically with many contradicting predictions.[1]

PAMAM dendrimers were the first type of dendrimer to be commercialized,[3] and due to both their availability and their promising potential for biomedical applications, solutions of PAMAM dendrimers in water have been the focus of intense research.[4] The vast majority of theoretical and experimental studies to date have focused on the changes of single-molecule structure of dendrimers as a function of different environmental variables.[5−10] However, less is known about the interdendrimer interactions in solutions, and this is a critical point for biomedical applications, since they require concentrated solutions. Additionally, there is no clear understanding of the role counterion association plays in modifying the structure and interaction of charged PAMAM in solution. Only recently, computational studies investigated the specific counterion association in these dendrimer solutions, but there is so far no experimental studies addressing this complex problem.[11]

Previously, we presented a method for investigating dendrimer structure in an aqueous environment with changing acidity using small-angle neutron scattering (SANS) along with a model built from statistical mechanics.[12] As an example, generation 4 PAMAM dendrimer was chosen for this study. In comparison to the predictions of various computational works, two quantitative disagreements were found in our experimental results: First the molecular size, characterized by the radius of gyration R_G, was seen to be essentially independent of molecular protonation when the pD value is adjusted within the range from 10 to 5. Moreover, we found that the number of associated counterions was significantly larger than the value predicted by MD simulations which incorporate the counterions explicitly. It is natural to relate the observed conformational invariance to the packing of associated counterions, which is mediated by the unique structural openness at the molecular level. However, there is still lack of study of the counterion association effect in dendrimers systematically with different generations.

Recently, there has been also considerable attention given to study the structural properties of PAMAM dendrimer using optical probe techniques.[13,14] It has been found that, within a certain pH range, a fluorescence emission from PAMAM dendrimer solutions was observed with a surprisingly strong generational dependence. This effect has been conjecturally attributed to the different degree of charged interacting groups

* To whom correspondence should be addressed. E-mail: chenw@ornl.gov.
† Institut Laue-Langevin.
‡ National Institute of Standards and Technology.
§ University of Maryland.
|| The Center for Nanophase Materials Sciences, Oak Ridge National Laboratory.
⊥ University of Tennessee.
Spallation Neutron Source, Oak Ridge National Laboratory.

10.1021/jp805297a CCC: $40.75 © 2008 American Chemical Society
Published on Web 10/25/2008

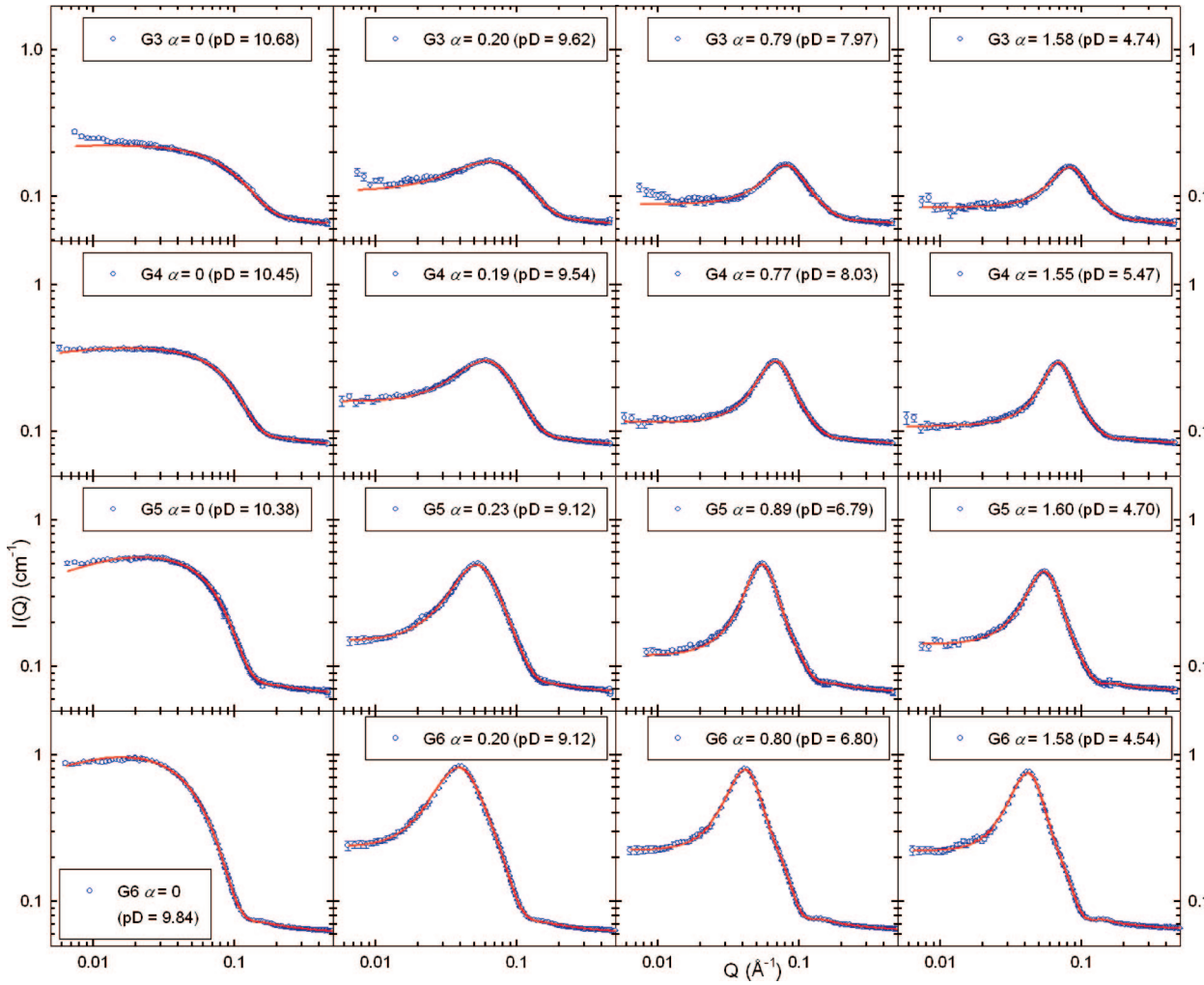

Figure 1. SANS spectra selected from the series of G3, G4, G5, and G6 PAMAM dendrimers in D_2O solutions with a fixed dendrimer weight fraction of 0.0225 g/mL for four different α values (0, 0.2, 0.8, and 1.6, respectively) and the theoretical model fits (red lines).

among the constitute components of dendrimer and associated counterion.[14] At present, the exact physical mechanism remains unclear.

In this report, we are aiming to explore the effect of dendrimer generation on counterion condensation via a systematic study of the generation 3−6 (G3−6) dendrimer in aqueous solutions by small-angle neutron scattering. It is found that for any generation, upon increasing the molecular protonation, the molecular size, quantified by the radius of gyration, R_G, is essentially independent of the variation of the pD of the solutions although there seems to be some changes in the intra-dendrimer structure. A strong dependence of counterion association with the dendrimer generation is also observed which results in a moderate increase of the effective charge as the generation number increases. This observation is intrinsically different from recent computer simulation which predicts an exponential increase of effective charge as a function of the generation number.[15]

II. Materials and Small-Angle Neutron Scattering

The PAMAM dendrimers used in this work were purchased from Dendritech Inc., Midland, MI.[16] Deuterium chloride (catalog number DLM-54-25) and deuterium oxide (catalog number DLM-6-10X1) were obtained from Cambridge Isotope Laboratories, Inc., Andover, MA.[16] The samples were prepared by dissolving PAMAM dendrimer in solutions of DCl and D_2O; the preparation of the samples studied in this investigation is described in a separate reference.[12] The total amount of amines contained in each sample is kept at a constant value by fixing the dendrimer concentration at 0.0225 g/mL. The METTLER TOLEDO S20 SevenEasy pH meter[16] was used to extract the pD, which is converted by the reading of the pH meter according to a generally accepted relation pD = pH + 0.41.[12] Furthermore, the deuteron concentration is corrected from the measured deuteron activity.[17]

The concentration of acid added is represented by the acidity scale factor α, which is defined as the molar ratio of acid to primary amines

$$\alpha \equiv \frac{[\mathrm{DCl}]}{[-\mathrm{NH_2}]} = \frac{[\mathrm{DCl}]}{2^{n+2}[\mathrm{PAMAM}]} \tag{1}$$

where n is the dendrimer generation. The samples are prepared with different α values ranging from 0 to 1.8, with the corresponding pD values ranging roughly from 10.4 to 5. Right after sample preparation, the SANS measurements were carried out using the NG3 SANS spectrometer at the NCNR NIST. The wavelength of the incident neutron beam was chosen to be 6.0 Å, with a wavelength spread $\Delta\lambda/\lambda$ of 15%, to cover values of the scattering wave vector Q ranging from 0.0045 to 0.45 $Å^{-1}$. The measured intensity $I_{exp}(Q)$ was corrected for detector

background and sensitivity and for the scattering contribution from the empty cell and placed on an absolute scale using a direct beam measurement.[18] All the experiments were carried out at a controlled temperature of 23.0 ± 0.1 °C.

In this study, $I_{exp}(Q)$ is modeled by the following integral equation

$$I_{exp}(Q) = \int_0^\infty \frac{I_{model}(z)}{\sqrt{2\pi\delta(Q)^2}} \exp\left[-\frac{(z - Q_m)^2}{2\delta(Q)^2}\right] dz \quad (2)$$

where $I_{model}(Q)$ is the theoretical intensity distribution, $\delta(Q)$ the width of the resolution function at Q, and Q_m is the mean Q value.[18] We only briefly outline the major elements of $I_{model}(Q)$ with details reported in ref 12.

In our approach, the coherent scattering of PAMAM solutions is modeled by the factorization approximation which is valid for describing the small-angle scattering intensity distribution obtained from the colloidal systems consisting of monodispersed spherical particles:[19] The $I_{model}(Q)$ is in principle proportional to the scattering contrast between dendrimers particle and the solvent, the normalized form factor $P(Q)$, and the structure factor $S(Q)$. $P(Q)$ is given by the fuzzy ball model[12]

$$P(Q) = \left\{\frac{3}{(QR)^3}[\sin(QR) - QR\cos(QR)]\exp\left(-\frac{Q^2\sigma^2}{4}\right)\right\}^2 + a_b P_{fluc}(Q, R_G) \quad (3)$$

The convolution of a hard sphere with radius R and a Gaussian with variance σ^2, given in the first term on the right-hand side of eq 3, is used to approximate the dense core nature and the diffuse interface of the PAMAM molecule.[12,31] The second term is introduced to incorporate the scattering contribution from the intradendrimer density fluctuations dominating the high Q region, with a_b giving the ratio of its contribution to $P(Q)$ normalized to the first term.

$S(Q)$ is obtained by numerically solving the Ornstein−Zernike integral equation (OZ) for a one-component system in combination with the hypernetted chain (HNC) closure,[20] which has been demonstrated to give an accurate description of the spatial arrangement of the charged colloidal suspensions by standard NVT canonical ensemble Monte Carlo simulations.[21] The effective inter-dendrimer interaction is approximated by the screened Coulombic interaction potential (Yukawa potential) along with a hard-sphere repulsive potential incorporated into our OZ-HNC approach. The effective diameter for a dendrimer is chosen as $2R_G$, consistent with the previous findings.[12] The essential physical quantities characterizing the charged PAMAM solutions, such as the effective charge carried by a single PAMAM dendrimer and the ionic strength, are converted from the fitted potential parameters based on the generalized one-component macroion approach (GOCM).[22,23] The deuteron concentration used in this work is corrected from the measured deuteron activity based on the theory originally proposed by Pitzer.[17]

III. Results and Discussion

Figure 1 gives the SANS scattering intensity distributions obtained from generation 3 to 6 (G3−G6) PAMAM solutions as a function of the acidity scale factor α. Qualitatively similar features are observed: For α = 0 the SANS curves present a plateau at small wave vectors reflecting noninteracting PAMAM dendrimer in solution. An interaction peak arises with increasing values of α, reflecting the enhanced interdendrimer Coulomb repulsion as a consequence of the protonation of the amines. The interaction peak remains unchanged within a broad range of α values from 1 to 1.8, which has also been observed in G4 solutions, and its possible reasons are discussed in ref 12. In some cases (mostly for G3), $I(Q)$ shows an slight upturn for $Q < 0.01$ Å^{-1}, characteristic of some aggregate as previously observed for these PAMAM.[24,25]

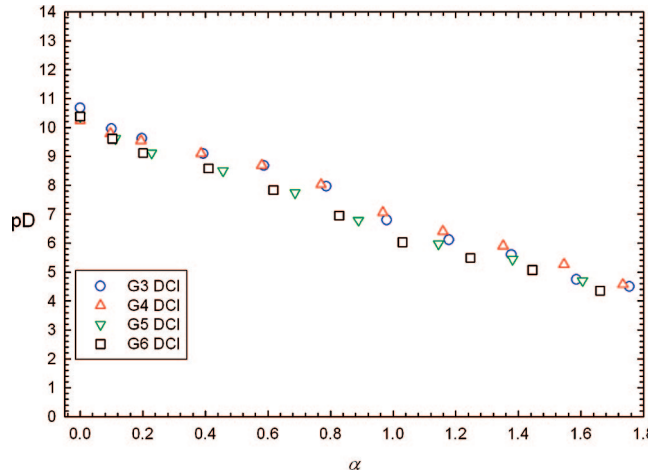

Figure 2. pD value of PAMAM dendrimers of generation 3, 4, 5, and 6 in D_2O solutions with concentration of 0.0225 g/mL as a function of α using DCl.

The measured pD as a function of α is presented in Figure 2. A steady decrease of pD as α increases from 0 to 1.8 is clearly seen, which is independent of the dendrimer generation and consistent with previous titration experiment.[26,27]

In molecular dynamic investigations the radius of gyration R_G is commonly calculated to parametrize the variation of the molecular conformation due to protonation of the amines. In our model, R_G is parametrized by the following mathematical expression:[12]

$$R_G = \sqrt{\frac{3}{10}(2R^2 + 5\sigma^2)} \quad (4)$$

where R is the radius of the analogous homogeneous sphere and σ the parameter characterizing the soft shell region. Both quantities are extracted from model fitting.[12]

As shown in Figure 3, only a slight increase in R_G is found with increasing α for all four generations of PAMAM dendrimers studied (about 7% for G3, 4% for G4, 5% for G5, and 5% for G6) within the studied pD range. Quantitatively, these results are not consistent with an extensive number of computational studies which have repeatedly concluded that charging the amines in PAMAM dendrimer should result in a substantial increase in R_G.[28] However, a similar experimental observation has been reported for G8 PAMAM dendrimer before.[29] In our case, by taking into consideration the structure factor explicitly, the value of R_G can be determined in a more quantitatively rigorous manner compared to a rather limiting high Q data fit with a form factor $P(Q)$ model, such as the approach adopted in ref 29. However, it is not possible for the mean-field model used in our SANS data analysis to provide any atomic-level mechanism to interpret the disagreement between our SANS experimental results and the MD predictions. It has been

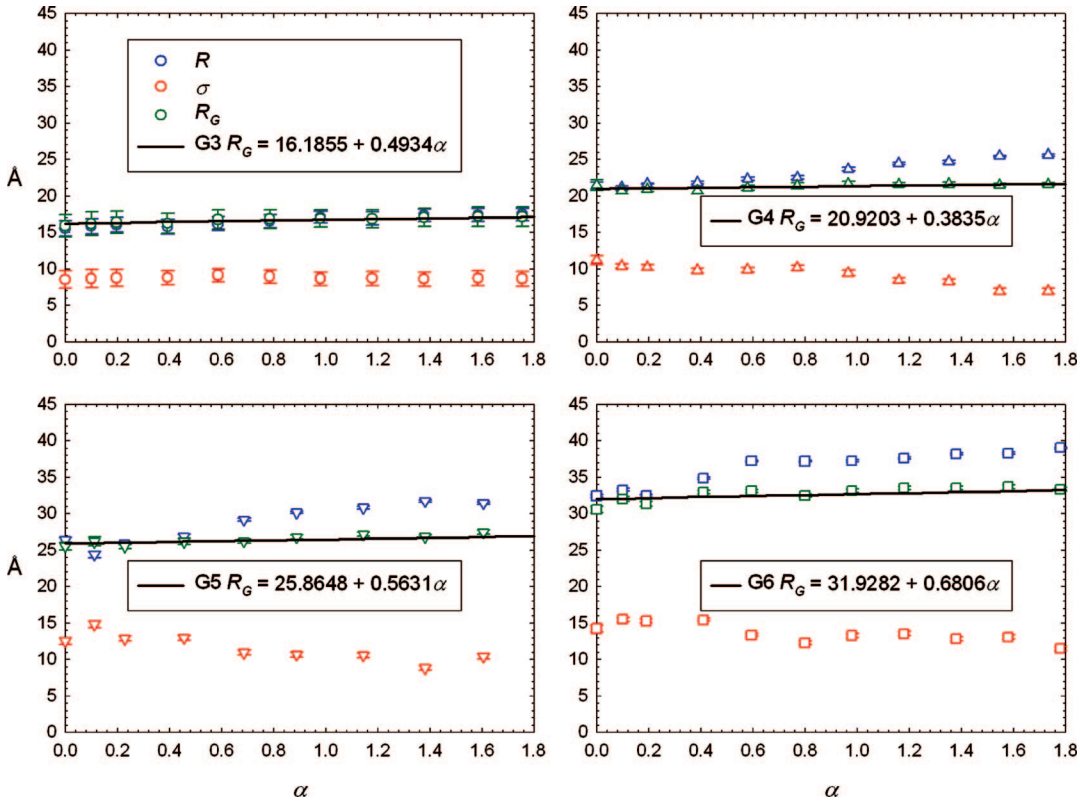

Figure 3. Variation of the intradendrimer structure factor $P(Q)$ parameters R, σ, radius of gyration R_G, and the corresponding calibration curves as a function of α. In the four generations studied in this work, as indicated by the empirical fitting, SANS model fitting reveals a moderate expansion of R_G when the solutions are increasingly acidified.

conjectured that this observed insensitivity of R_G to molecular protonation in G8 PAMAM solutions was due to the extremely strong steric crowding between branches in higher generation of dendrimers.[1] However, our findings for different generations of PAMAM dendrimers clearly indicate that this insensitivity is a *common feature* shared by lower generation dendrimers as well and suggest that packing constraints alone cannot account for this effect in small dendrimers with a much more open molecular architecture. A possible explanation from thermodynamical mean-field calculations[9,30] suggests that the repulsion among charged amines of PAMAM dendrimers is further offset by extra screening introduced by the high internal counterion concentration due to the confinement effect. This direct analogy with the behavior observed for charged diamine molecule is responsible of a weak dendrimer molecular size dependence with charge. This point is also backed by the recent titration experiments,[26,27] which conclude that proton−amine binding constant, and repulsions among protonated amines are significantly modulated by the microenvironment within the dendrimer interior.

Despite a nearly constant R_G, a dependence of the intramolecular structure on protonation is found and can be observed most clearly by plotting the ratio σ/R as a function of α (Figure 4). On the basis of the fuzzy ball picture,[12] protonation of the PAMAM amines results in a transformation of the dendrimer molecular density profile from a more diffusive density distribution in the neutral state to a more uniform, hard-sphere-like configuration when the amines are progressively charged. This was previously observed in G4 PAMAM solutions, and here similar results are obtained for G5 and G6 PAMAM as well. It is sensible to attribute this observed change in the molecular density profile to the combined effect of protonation of amines and counterion condensation enhanced by the unique intramolecular structure. There seems to be a similar change upon charging the G3 dendrimers. However, due to its relatively small size, the quality of the SANS spectrum obtained from the G3 solutions does not allow us to extract conclusive assertion, and therefore the trend of the pD-dependent transformation observed for the higher dendrimer generation is much less obvious for G3. Moreover, the evolution of the molecular density profile of G4−6 dendrimer as a function of protonation is characterized by the same quantitative feature: despite the expected difference in the intramolecular architecture for dendrimers of different

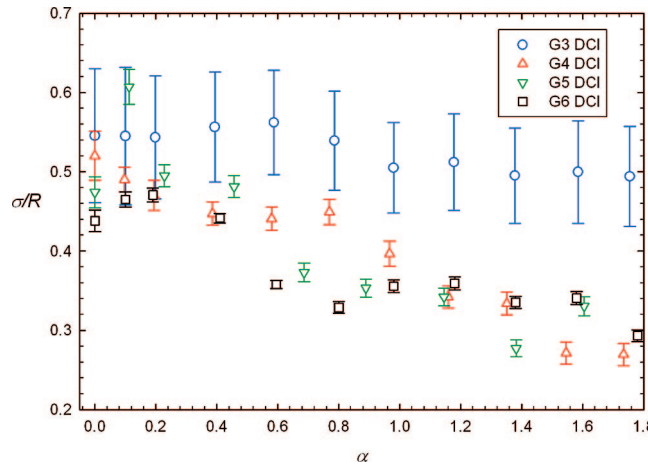

Figure 4. Variation of the value of σ/R as a function of α for the different PAMAM generations. Despite of the overall insensitivity of R_G to the changes of pD of solutions, the progressively increase of the molecular protonation triggers a transition of the intramolecular density profile from a diffusive profile to a more uniform one, as indicated by a decrease value of σ/R. The smaller size of G3 PAMAM results in a lower signal-to-noise ratio in the measurements and consequently more uncertainty in the resulting fitting parameters.

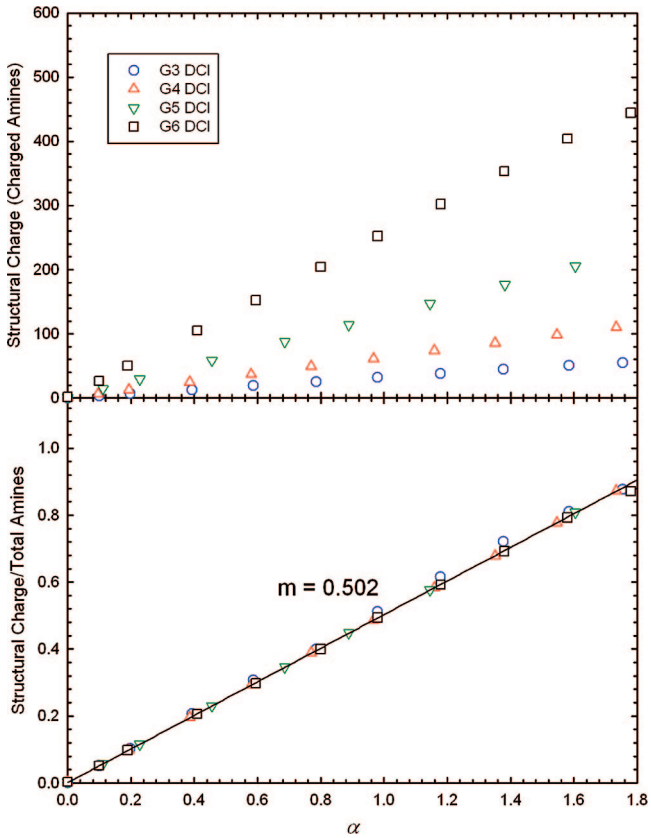

Figure 5. Top panel: numbers of the structural charge, namely the total charged amines, as a function of α for G3 to G6 PAMAM dendrimers in D_2O solutions are given in the top panel. The values are calculated from the macroscopic charge neutrality incorporating the correction of the deuteron activity. Error bars are smaller than the symbol size. Bottom panel: charged amines for different generations normalized to their respective total number of amines as a function of α. It is evident that all the calibrated curves collapse into one single master curve. The degree of molecular protonation is seen to increase almost linearly with a slope of about 0.5 within the range of $0 < \alpha < 1.8$.

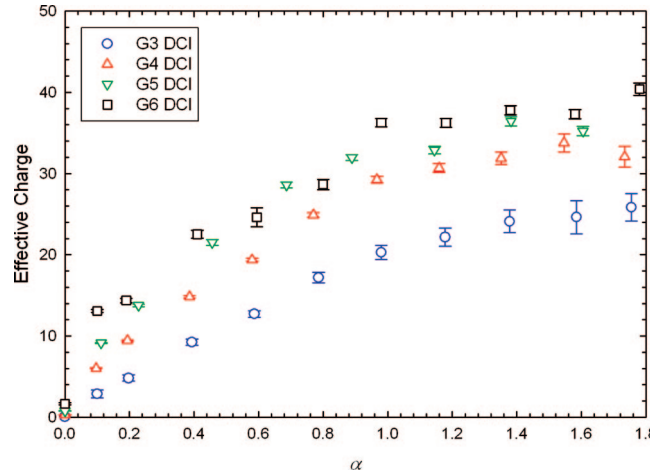

Figure 6. Effective charges carried by a dendrimer molecule obtained from the SANS model fittings as a function of α. The effective charge steadily increases at low α and show a weak dependence on α for $\alpha > 1$.

generations,[31] the ratio of σ/R becomes nearly identical once they are fully charged.

The total number of protonated amines, namely the structural charge in the language of colloidal science, can be obtained by applying the constraint of macroscopic charge neutrality (Figure 5). For all the generations studied, with increasing α, the molecular protonation increases nearly linearly at low α up to α values of ~1.8. The number of charged amines for all generations PAMAM falls onto a single curve when normalized by the total number of amines present (Figure 5, bottom panel). This observation suggests that the pairing between the deuteron and the amine is not affected by the expected difference in intramolecular microenvironment for dendrimers of different generations. The curve shows the expected slope of 0.5 because approximately half of the amines are primary, which are known to have a higher pK_a and therefore acquire charge before the tertiary amines become charged.[26,27]

The effective charge carried by a single dendrimer molecule is the difference between the number of charged amines and the number of associated chlorides and is directly extracted from the SANS intensity fit. For all the generations studied, two distinct regimes are observed in the α-dependence of the effective charge (Figure 6). At low α values ($\alpha < 1$), where only the primary amines are charged, the effective charge increases linearly. At larger values of α ($\alpha > 1$), the tertiary amines start to be protonated, but the effective charge shows only a very weak dependence on α. Over the entire range of α studied in this report, the effective charge shows a generational dependence, with larger dendrimers acquiring a higher effective charge. However, this generational effect is less substantial for higher generation of dendrimers. The increase in effective charge from G5 to G6 PAMAM at $\alpha > 1$ is smaller compared to the difference in effective charge between G4 and G5 PAMAM, and the largest difference is observed between G3 and G4. Despite the large number of the protonated amines per dendrimer molecule, the effective charge of a dendrimer saturates only at about 24, 30, 35, and 40 for G3, G4, G5, and G6 dendrimer, respectively, instead of increasing exponentially as predicted by a very recent computational work.[15] The invariance of the effective charge at $\alpha > 1$ implies that when tertiary amines are charged, each charged tertiary amine group can only attract one counterion inside a dendrimer. At present, it is still not clear whether this is due to the effect of the space limit or the specific binding effect.

Further, a strong generational dependence of counterion condensation is observed: Upon increasing the degree of molecular protonation, a progressive increase amount of chloride association is observed (Figure 7). It is not surprising that, going from lower generation charged dendrimer to the higher one, the average number of associated counterions *per molecule* increases due to the linear increase of the total structural charge with the same degree of molecular protonation as shown in Figure 5.

With the values of the molecular parameters obtained from SANS model fitting, we can estimate the density of associated chloride ion in a dendrimer: It is noticed that there are $2^{(n+3)} - 2$ amines, including both primary and tertiary ones, in a PAMAM dendrimer of generation n. It has been shown, by our current model fitting results and the computational work,[7] that R_G increases almost linearly upon increasing n. Hence, for a given generation n, the molecular volume of a dendrimer is expected to be proportional to n^3. Assuming the intramolecular space occupied by a single primary amine and tertiary one is identical, the internal volume per amine V_A is therefore proportional to $n^3/[2^{(n+3)} - 2]$, which is 0.44, 0.51, 0.49, and 0.42 for G3, G4, G5, and G6, respectively. From our estimation the amine density is found to reach a minimum at G4 dendrimer and increase when $n > 4$. The calculated number of associated

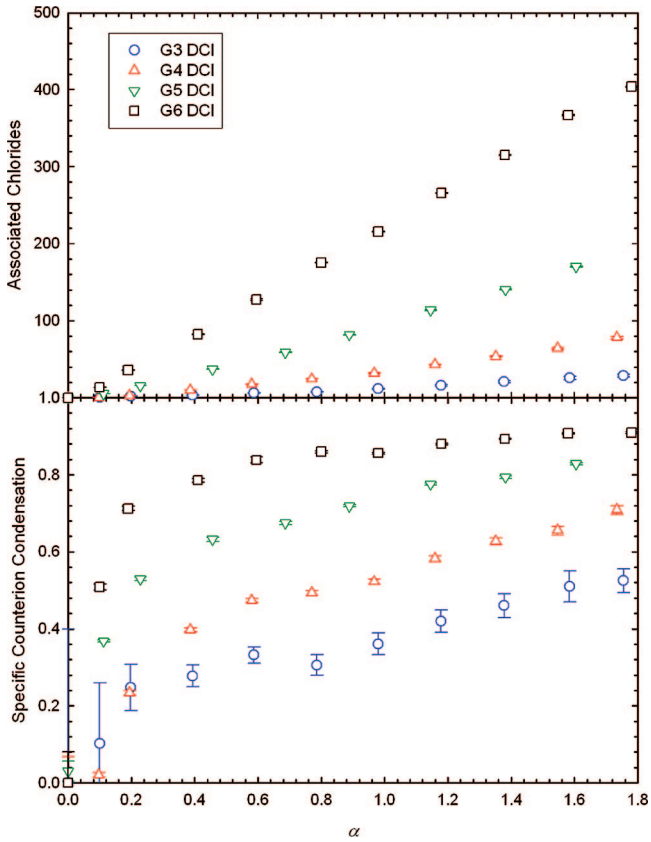

Figure 7. As shown in the top panel, the associated number of chlorides exhibits a similar pD-dependent behavior as the molecular protonation (Figure 5). The bottom panel presents the specific counterion condensation, defined as the number of the associated chlorides divided by the number of the charged amines, as a function of α. A strong dependence on generation is clearly observed: With the same condition of molecular protonation, the degree of chloride association is seen to increase considerably from lower generation charged PAMAM dendrimer to the higher ones.

counterions *per amine* (Figure 7, bottom panel), defined by us as *specific counterion condensation*, is clearly shown to increase steadily with advancing dendrimer generation. As an example, for G6 PAMAM at $\alpha = 1.8$, the specific counterion condensation is greater than 0.9; however, this ratio only reaches 0.5 for G3 PAMAM. The counterion density, which is proportional to the ratio between the specific counterion condensation and n^3, keeps increasing upon increasing the dendrimer generation.

This generational dependence of specific counterion condensation and associated counterion density is certainly not intuitively predictable, and computation-wise it remains as a controversial issue at present: For example, Goddard et al.[7] predict a decrease in specific counterion condensation with increasing dendrimer generation. However, a increasing trend is seen by other simulation works, such as the one from Buzza et al.,[9] which is intrinsically different from Goddard's conclusion.

On the basis of the evidence provided by titration experiment[26,27] and thermodynamical mean-field theory,[9,30] we propose a hypothesis for this generation-dependent characteristic in counterion association: Given the same level of molecular protonation, the number of the chlorides associated with dendrimers increases steadily with each advancing generation. Here we argue the possible reason for this observation is due to their unique intramolecular structure: For PAMAM dendrimer, it has been shown that the molecular density profile is significantly modified by the backfolding of the constituent branches.[1] Therefore, it is consistent with the intuitive expectation that local density inhomogeneity is being developed simultaneously within the dendrimer interior. The amines, once being charged, are therefore able to form the inhomogeneously distributed potential wells to encapsulate the oppositely charged counterions, which is commonly found in many polyelectrolyte systems.[32] Because of the hierarchical nature of the structure, it is reasonable to say that this spatial inhomogeneity is developed in a generation-dependent manner. This speculation is not without any physical basis: As mentioned in the previous paragraph, it has been pointed out by titration experiments that the localization of the counterion association is greatly mediated by the interaction between the confined chlorides and the dendrimer local microenvironment, which has been known to be generational variable.[26,27] Consequently, the generational dependence of specific counterion condensation is manifested. Moreover, our report of this strong generational dependence of the association of chlorides with charged amines is consistent with predictions made by recent MD simulations.[9,10]

IV. Conclusions

We used a combined experimental and theoretical approach to investigate the structural changes in a generational series of PAMAM in acidified, aqueous solution, and we extracted the relevant molecular parameters. Along with a discernible change in the intramolecular density profile from a diffuse structure at neutral pD to a hard-sphere-like conformation in acidic environments, we find that there is no significant change in the radius of gyration R_G upon protonation of the dendrimer, which contradicts the predictions of most of MD simulations but is consistent with a previous SANS experiment for G8 PAMAM dendrimer[29] and mean-field calculations.[9,30] It is instructive to note that our findings from the SANS experiment of lower generation dendrimers suggests that the weak dependence of molecular size on protonation is an intrinsic structural nature of PAMAM dendrimer, instead of attributing it to the geometric constraint which is only pronounced in higher generation dendrimer.

We also found that the degree of counterion condensation is characterized by a strong generational dependence: The specific chloride condensation, defined as the average number of chloride associating one single charged amine, is seen to be higher for larger generation PAMAM dendrimers. The generation dependence of the effective charge differs from the recent computer simulation prediction[15] despite the agreement of the effective charge value at charged G4 dendrimer between our results and the simulation.

Acknowledgment. We gratefully acknowledge the support from the Laboratory Directed Research and Development Program (Project ID 05125) of ORNL and the partial financial support by U.S. Department of Energy within the Center of Excellence on Carbon-based Hydrogen Storage Materials. The support of the National Institute of Standards and Technology, U.S. Department of Commerce, in providing the neutron research facilities supported under NSF Agreement DMR-0454672 is also acknowledged. Part of this research was done at Oak Ridge National Laboratory's Center for Nanophase Materials Sciences which was sponsored by the Scientific User Facilities Division, Office of Basic Energy Sciences, U.S. Department of Energy.

References and Notes

(1) Ballauff, M.; Likos, C. N. *Angew. Chem., Int. Ed.* **2004**, *43*, 2998–3020.

(2) Meijer, E. W.; van Genderen, M. H. P. *Nature (London)* **2003**, *426*, 128–129.
(3) Tomalia, D. A.; Baker, H.; Dewald, J.; Hall, M.; Kallos, G.; Martin, S.; Roeck, J.; Ryder, J.; Smith, P. *Polym. J.* **1985**, *17*, 117–132.
(4) Tomalia, D. A. *Chem. Today* **2005**, *23*, 41–45.
(5) Welch, P.; Muthukumar, M. *Macromolecules* **1998**, *31*, 5892–5897.
(6) Lee, I.; Athey, B. D.; Wetzel, A. W.; Meixner, W.; Baker, J. R. *Macromolecules* **2002**, *35*, 4510–4520.
(7) Maiti, P. K.; Çaŭn, T.; Lin, S.-T.; Goddard, W. A. *Macromolecules* **2005**, *38*, 979–991.
(8) Maiti, P. K.; Goddard, W. A. *J. Phys. Chem. B* **2006**, *110*, 25628–25632.
(9) Giupponi, G.; Buzza, D. M. A.; Adolf, D. *Macromolecules* **2007**, *40*, 5959–5965.
(10) Karatasos, K. *Macromolecules* **2008**, *41*, 1025–1033.
(11) Likos, C. N.; Ballauff, M. *Top. Curr. Chem.* **2005**, *245*, 239–252.
(12) Chen, W.-R.; Porcar, L.; Liu, Y.; Butler, P. D.; Magid, L. J. *Macromolecules* **2007**, *40*, 5887–5898.
(13) For example, see: Shcharbin, D.; Klajnert, B.; Mazhul, V.; Bryszewska, M. *J. Fluoresc.* **2003**, *13*, 519.
(14) See: Wang, D.; Imae, T.; Miki, M. *J. Colloid Interface Sci.* **2007**, *312*, 8–13, and references therein.
(15) Maiti, P. K.; Messina, R. *Macromolecules* **2008**, *41*, 5002–5006.
(16) In their own activities as scientific institutions, NIST and ORNL use many different materials, products, types of equipment, and services. However, NIST and ORNL do not approve, recommend, or endorse any product or proprietary material.
(17) Pitzer, K. S. In *Activity Coefficients in Electrolyte Solutions*, 2nd ed.; Pitzer, K. S., Ed.; CRC Press: Boca Raton, FL, 1991.
(18) Kline, S. R. *J. Appl. Crystallogr.* **2006**, *39*, 895–900.
(19) Chen, S.-H. *Annu. Rev. Phys. Chem.* **1986**, *37*, 351–399.
(20) Hansen, J.-P.; McDonald, I. R. *Theory of Simple Liquids*, 3rd ed.; Academic Press: Amsterdam, 2006.
(21) For example, see: Broccio, M.; Costa, D.; Liu, Y.; Chen, S.-H. *J. Chem. Phys.* **2006**, *124*, 084501–9.
(22) Belloni, L. *J. Chem. Phys.* **1986**, *85*, 519–526.
(23) Chen, S.-H.; Sheu, E. Y. In *Micellar Solutions and Microemulsions - Structure, Dynamics, and Statistical Thermodynamics*; Rajagopalan, R., Chen, S.-H., Eds.; Springer: New York, 1990.
(24) Ramzi, A.; Scherrenberg, R.; Joosten, J.; Lemstra, P.; Mortensen, K. *Macromolecules* **2002**, *35*, 827–833.
(25) Pötschke, D.; Ballauff, M.; Lindner, P.; Fischer, M.; Vögtle, F. *Macromolecules* **1999**, *32*, 4079–4087.
(26) Niu, Y.; Crooks, R. M. *Macromolecules* **2003**, *36*, 5725–5731.
(27) Cakara, D.; Kleimann, J.; Borkovec, M. *Macromolecules* **2003**, *36*, 4201–4207.
(28) See Opitz, A. W.; Wagner, N. J. *J. Polym. Sci., Part B: Polym. Phys.* **2006**, *44*, 3062–3077, and references therein.
(29) Nisato, G.; Ivkov, R.; Amis, E. J. *Macromolecules* **2000**, *33*, 4172–4176.
(30) Govorun, E. N.; Zeldovich, K. B.; Khokhlov, A. R. *Macromol. Theory Simul.* **2003**, *12*, 705–713.
(31) Rathgeber, S.; Monkenbusch, M.; Kreitschmann, M.; Urban, V.; Brulet, A. *J. Chem. Phys.* **2002**, *117*, 4047–4062.
(32) Zeldovich, K. B.; Khokhlov, A. R. *Macromolecules* **1999**, *32*, 3488–3494.

JP805297A